Canadian Journal of Zoology

Research Article

Gastropod shell differentiation following colonization of an invasive intertidal macrophyte in Atlantic Canada

T.E. Reimchen, J. Holden, and A.R.B. Cortese

Dep't of Biology, University of Victoria, PO Box 1700, Victoria, BC V8W 2Y2, Canada

Corresponding author: **T.E. Reimchen** (email: reimchen@uvic.ca)

Abstract

In the 19th century, a lower intertidal macrophyte, *Fucus serratus* (Linnaeus), from western Europe was introduced to Nova Scotia, Canada, where it successfully established, co-existing with native macrophytes *Fucus vesiculosus* (Linnaeus) and *Ascophyllum nodosum* (Linnaeus). We first examined whether a common gastropod in Nova Scotia, *Littorina obtusata* (Linnaeus, 1758), which grazes on the native macrophytes, has exploited the invasive and on finding this, we secondly examined whether there has been any phenotypic differentiation on the invasive. Among 98 sites surveyed around Nova Scotia and Newfoundland in May and June 1994, 11 had the invasive macrophyte, all of which showed colonization by *L. obtusata* including egg masses, juveniles, and adults. Among 2135 shells photographed for digital image analyses, those on the invasive differed from those on the native macrophytes with respect to (1) RGB (red/green/blue) channels, (2) HSV (hue, saturation, brightness) phenotypes, (3) protoconch pattern, and (4) adult shell size. Nitrogen and carbon stable isotope signatures on muscle tissues from a subset of *L. obtusata* indicate foraging fidelity on the invasive rather than temporary occupation. We suggest that these cumulative phenotypic responses to the invasive macrophyte that vary in extent and direction within and among localities reflect localized adaptation and offer a unique opportunity for quantifying early stages of phenotypic and genomic differentiation in a novel ecological niche.

Key words: invasive species, *Fucus serratus*, *Littorina obtusata,* shell color, shell size, stable isotopes

Introduction

Introduction of invasive species, an increasingly common event across the globe, is known to substantially alter biotic interactions and facilitate phenotypic/evolutionary changes in native species (Levine et al. 2003; Callaway and Maron 2006; Strauss et al. 2006; Dijkstra et al. 2017; Van Volkom et al. 2021). The western European intertidal macrophyte, *Fucus serratus* (Linnaeus), was inadvertently introduced to the temperate western Atlantic in about 1870 and has subsequently spread along the northern shores of Nova Scotia and Prince Edward Island where it co-exists with two native macrophytes, *Fucus vesiculosus* (Linnaeus) and *Ascophyllum nodosum* (Linnaeus) (Edelstein et al. 1973; Johnson et al. 2012; Garbary et al. 2021). In the eastern Atlantic, *F. serratus* extends from the low to the mid-intertidal where it overlaps with the mid-intertidal macrophytes, *F. vesiculosus* and *A. nodosum*. While there is horizontal overlap of the macrophytes when the tide is at its lowest, during full submergence at high tide, the flat *F. serratus* fronds remain on the substrate while *F. vesiculosus* and *A. nodosum* project vertically into the water column due to buoyancy of the gas vesicles in their fronds. Dominant grazers on these macrophytes are gastropods. The most common is *Littorina obtusata*, found in both the eastern and western Atlantic, and is generally found on *F. vesiculosus* and *A. nodosum*. An additional periwinkle, *Littorina fabalis* (Turton, 1825) (formerly *L. mariae* (Sacchi and Rastelli, 1966)), and a sibling of *L. obtusata*, is found only in the eastern Atlantic and is largely restricted to the lower intertidal *F. serratus* (Fig. 1).

These sibling species of periwinkles are phenotypically and genetically distinctive (Sacchi 1969; Reimchen 1974, 1979, 1981, 1982; Goodwin and Fish 1977; Watson and Norton 1987; Williams 1994, 1995; Marques et al. 2017; Sotelo et al. 2020). In the United Kingdom (UK) and Ireland, adult shell size of *L. obtusata* is generally twice as large as *L. fabalis* (Reimchen 1981, 1982), while their shell color is usually light to dark olive compared with yellow or dark brown for *L. fabalis* (Reimchen 1974, 1979). Protoconch color of *L. obtusata* is usually opaline (weakly pigmented), yet for *L. fabalis* the protoconch is often opaque white or dark brown (Reimchen 1989). Based on field surveys and collections in May and June 1994, we examine whether *L. obtusata* has colonized the invasive macrophyte in Atlantic Canada and if so, assess whether it exhibits any shell color or size differentiation from conspecifics on native *F. vesiculosus* and *A. nodosum* in the direction of the *L. fabalis* phenotype, which is absent from the western Atlantic. We quantify five attributes of *L. obtusata*: (1) the relative abundance on the different macrophytes, as this would provide a general proxy for grazing preference; (2) age and size class (juvenile/adult), assuming that the presence of juveniles on the

Fig. 1. Infographic of simplified intertidal zonation at high tide showing common macrophytes and common grazing periwinkles (*Littorina obtusata, L. fabalis*) for the eastern and west Atlantic. Only most common shell colors of periwinkles shown. Shell sizes of the two periwinkles in the eastern Atlantic are not to scale with respect to the macrophytes but are to scale relative to each other. Note that *Ascophyllum nodosum* and *Fucus vesiculosis* project into the water column (due to the gas bladders), while *F. serratus* (no bladders) lies on the substrate. *F. serratus* was not present in the western Atlantic prior to ~1870. Common coloration of *L. obtusata* and *L. fabalis* shells for the eastern Atlantic extracted from Reimchen (1974). Common coloration of *L. obtusata* shell from the western Atlantic extracted from Phifer-Rixey et al. (2008).

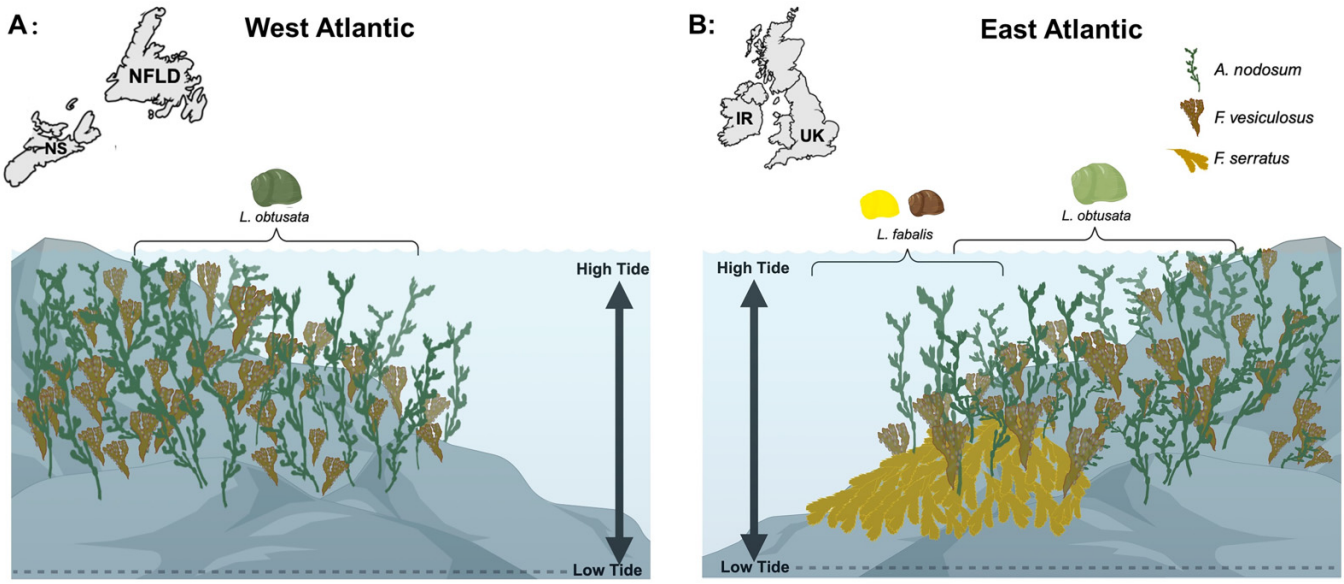

invasive would be consistent with egg-laying by this direct-developing littorine; (3) adult shell size, as we expected that this would be smaller on *F. serratus* relative to those on *F. vesiculosus* and *A. nodosum*; (4) color of the major shell whorl, expecting that there would be a reduction in olive phenotypes and a shift towards yellow or brown phenotypes on the invasive macrophyte. For shell color, we use digital imaging to quantify color space including red, green, and blue channels (RGB) and hue, saturation, and brightness (HSV) as this allows greatly improved color classification relative to the customary visual binning into several phenotypic categories (eg. Endler 1991; Sacchi et al. 2013; Valvo et al. 2021), (5) color of the protoconch (shell apex), as this is a useful predictor of microhabitat of the juvenile snails (Reimchen 1989), and (6) nitrogen and carbon stable isotopes of the muscle tissues of the periwinkles to assess whether there is any isotopic differentiation of the periwinkles on the invasive relative to the native macrophytes.

Methods

Field collections

We made collections of *L. obtusata* on macrophytes from 98 localities in Nova Scotia and Newfoundland, Canada in May and June 1994. While *F. vesiculosus* and/or *A. nodosum* were present in all localities and were the dominant substrates of the periwinkle, *F. serratus* was found in only 11 localities, all in Nova Scotia (Fig. 2). At all localities, an intertidal area was initially chosen that had extensive algal cover. Within an approximate 10 m × 10 m area, collections were made of the snails from dominant macrophytes. Some localities also contained patches of *Fucus edentata* (Bachelot Pylaie) or *Fucus distichus* (Linnaeus) that we did not sample for the periwinkles. To minimize visual collecting bias of the often camouflaged snails, the algal fronds were rigorously shaken and all the snails were retrieved from the substrate beneath the fronds and preserved in 95% ethanol. Even after a decade, the alcohol preservative did not appear to the human eye to influence shell color. Although subtle fading is possible, this would not affect our analyses, which is to compare differences in shell color among algal species within the same locality. Relative abundance (1–5) of snails was approximated based on the sample size and effort. At each locality, we visually estimated relative cover of each macrophyte (uncommon < 20%; common 20%–70%; abundant > 70%), average frond length, average frond hue (light olive, olive, dark olive), major underlying substrate (mud/sand/rocks/bedrock), shoreline slope (<20°, 20–70°, >70°), and wave exposure (sheltered, moderate, and exposed).

Shell color and shell size determination

Because the color of shells appeared to visually grade from light yellow through to dark brown (see Fig. 3A) and could not be assigned to discrete morphs, we used photographs to quantify color digitally. For each sample, 35 snails (if available) were placed on a tray on a defined grid with a scale bar (for shell size determination using "count colors," Weller 2019) and were submerged in water. A digital camera (Lumix DMC-ZX60) was mounted on a stand 35 cm directly above the

Fig. 2. Collection sites of *Littorina obtusata* containing two or more macrophyte species, including the invasive *Fucus serratus*. Putative 1870 introduction of *F. serratus* occurred at Pictou. The map was created with the R package "marmap" and "ggplot2."

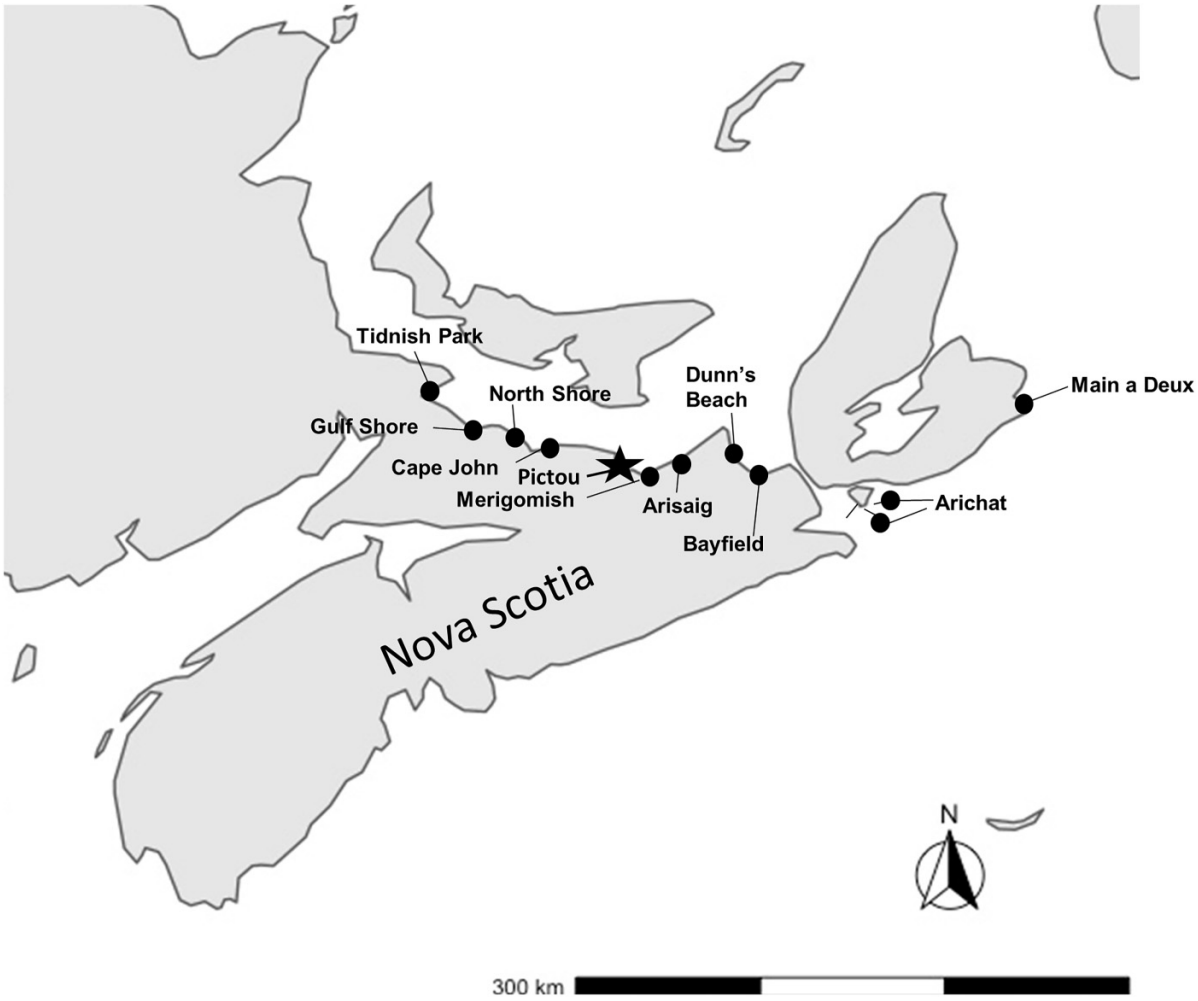

tray. Consistent lighting conditions were provided by a single 5000 K "bright white" bulb positioned 105 cm above and 72 cm to the right of the tray. A diffuser minimized light glare on the surface of the water. Digital images were obtained as 8-bit JPEG files (4896 x 3672 pixels) using consistent camera settings (aperture 4.3, shutter speed 1/13th, ISO 2000; focal distance 57 mm). White-balance settings were set as automatic because the light source and intensity were identical across all photos. In localities where larger sample sizes were available, additional snails (excluding juveniles) were processed using the same methods. A total of 2135 snails were photographed. Shell size was quantified on the digital images using the R-package "countcolors" (0.9.1; Weller 2019) and verified on a subset of samples using direct shell measurement with a caliper (details in Supplementary Text 1).

The digital image of each shell (557 × 520 pixels; 4 compressed bits per pixel) was extracted and the background surrounding the shell was digitally replaced with white pixels. Analyses were carried out using "colordistance" (1.1.2: Weller 2021) that allowed for representation and comparison of pixels in three-dimensional color spaces (RGB—red, green, and blue; HSV—hue, saturation, and brightness). For each snail image, individual pixels representing shell color were first plotted in the three-dimensional RGB color space with white background pixels excluded (lower bounds; RGB decimal value = 0.8, 0.8, 0.8 upper bounds; RGB decimal value = 1.0, 1.0, 1.0). A unique color histogram representing shell coloration was then obtained for each image by grouping pixels into eight three-dimensional bins (3 color channels, 2 bins per channel) within the RGB color space. From this, a mean RGB value was provided for each histogram bin using RGB values from pixels within the respective bin, with bin size being proportional to all pixels present from the entire shell. HSV values were also collected for each snail image in an identical fashion as RGB values and used in later analysis. We then used the mean RGB value representative of the largest color bin to assign each snail a specific color within the Inter-Society Color Council and National Bureau of Standards (ISCC-NBS) color system (methods in Cox et al. 2021). Conversion of RGB values to a representative hexadecimal color code and unique name based on the Munsell color system were used to classify shell morphs for each shell image. We separately sorted all 267 of the defined ISCC-NBS color names as to their visual appearance being most compara-

Fig. 3. (A) Representative range of shell coloration within collected samples of *L. obtusata* from Nova Scotia and Newfoundland. (B) Spectral readings taken of representative periwinkles exemplifying differentiation between visible color morphs for visual spectra from 500 to 700 nm. A moving average of 50 was applied to curves with relative intensity standardized using Z-scores. (C) Field photographs of representative macrophytes including transmitted light through fronds for *F. serratus.*

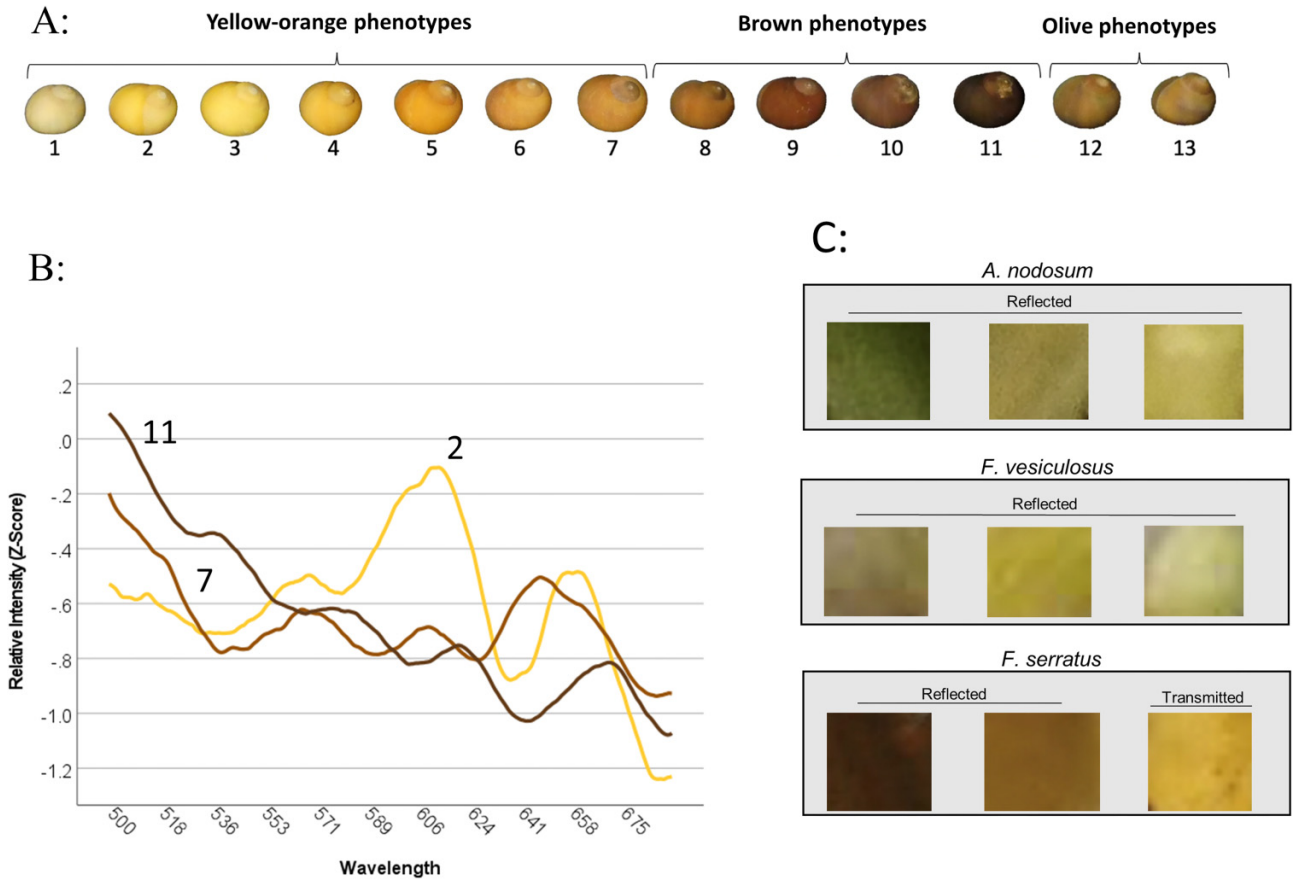

ble to tones of yellow-orange, olive, or brown. Since not all ISCC-NBS colors were representative of the naturally occurring range of *L. obtusata* shell colors (eg. vivid pink), only 171 unique color categories were used. Each snail was assigned to either a brown, olive or yellow-orange morph category. We then compared this digital classification to a visual classification of the shells that were consistent with the brown, olive or yellow-orange categories. For many individuals, coloration was not uniform across the entirety of the shell, in part due to abrasions. Therefore, we used only the largest color bin on the major whorl of each shell for digital analysis.

To provide an independent classification of shell color from the RGB/HSV analyses, we selected 13 *L. obtusata* specimens that encompassed the gradient of shell colors present (Fig. 3A) and made spectral reflectance measurements using an OceanOptics USB2000 spectrophotometer with a reflectance probe (Ocean Optics R200-7-UV/VIS) and a tungsten–halogen light source (Ocean Optics LS-1). Prior to each scan of the shell, a white reference was taken. The reflectance probe was placed 1 mm above the apex of each shell and measured (380–700 nm) with a 3 ms integration time, spectra average set to 10, and a boxcar width of 20. All snails were moistened with water immediately prior to taking a spectral reading. These data (Fig. 3B) were cross-referenced to their jpeg images that confirmed the RGB classifications. Photographs of the three macrophyte species obtained in the field show representative frond surfaces on which the snails are found (Fig. 3C).

There was often ontogenetic variability in shell color at the protoconch stage (early post-hatching) that could differ from the color characterizing most of the shell (images in Reimchen 1989). The digital images did not allow accurate color classification of the protoconch. As a result, on each shell ($N = 3991$), the apex was visually classified (under a dissecting microscope) into one of four categories: (1) same color as major shell whorl, (2) opaline to white (no evidence of any banding), (3) white-spiral band at mid-position of the protoconch whorl, and (4) not scored due to abrasion (primarily adult snails). We examined on the frequencies of the white-spiral phase on the different macrophytes.

Stable isotope data

We examined nitrogen and carbon stable isotopes of muscle tissues of *L. obtusata* from four localities. These isotopic data integrate longer term diet (3–8 months, Kemp et al. 1990; McIntyre and Flecker 2006) and potentially provide insight as to whether the snails were "resident" rather than "temporary" on the invasive macrophyte. In western Europe, intertidal macrophytes, including *F. serratus*, differ in sta-

ble isotope signatures, largely a consequence of locality effects rather than species effects (Viana and Bode 2013, 2015) and accordingly, individuals grazing on the different macrophytes could be expected to differ as well in their isotopic signatures. We extracted soft tissues from each of 184 periwinkles. The muscular foot was separated and placed in a drying oven at 60° for a minimum of 10 days and then powdered with a grinder. Approximately 1 mg of tissue (using an ATI CAHN-model C-44 scale) was packaged into D1002 5 × 3.5 mm pressed tin capsules for dual isotope analyses (^{13}C, ^{15} N). These were processed for isotope ratio mass spectrometry analysis at the Stable Isotope Facility at the University of California at Davis. Isotopic signatures ($^{\circ}/_{oo}$) were calculated from:

$$\delta 13C \text{ or } \delta 15N = [(\text{Rsample}/\text{Rstandard}) - 1] \times 1000$$

where R = the ratio of heavy to light isotopes.

Statistical analyses

Principle Component Analyses (PCA) were carried out to integrate the six shell color variables (R, G, B, H, S, and V). Differences in PC values among the macrophytes were compared with Analysis of variance (ANOVA). For comparison of dichotomous shell color classification (yellow-orange versus brown), we used contingency tests. To compare the extent of modality in the frequency distribution of shell hues on each macrophyte, we used Sarle's bimodality coefficient (Knapp 2007)

$$b = \left[\left(\gamma^2 + 1\right) / \left(\mathrm{k} + \left[\left(3(n-1)^2\right) / \left((n-2)(n-3)\right)\right]\right)\right]$$

where γ is skewness and k is kurtosis. Coefficients of 0 and 1 indicate a unimodal normal distribution and a full bimodal distribution, respectively. Values greater than 0.56 are considered statistical evidence for bimodal or multimodal distributions.

Adult shell size in these periwinkles is reached within 2 or 3 years and is characterized by development of a progressively thickened lip on the outer whorl, after which there is no increase in shell diameter. Because this progression to the maximum size and lip thickening is gradual, we used the five largest shells in each sample to approximate average maximum adult size as this best reflects the flattened slope of the asymptotic growth curve. Average shell sizes among the macrophytes were compared using Mann–Whitney U test.

Results

Among the 11 localities with *F. serratus*, all in northern Nova Scotia, relative density of periwinkles on the invasive *F. serratus* was marginally but not significantly lower than on the other macrophytes (*A. nodosum*, $\bar{x}$= 4.0, *F. vesiculosus*, $\bar{x}$ = 2.9, *F. serratus* $\bar{x}$ = 2.5, $F_{[2,113]} = 0.5$, $P = 0.6$). However, young periwinkles (thin-lipped) were significantly less common on *F. serratus* than on the two other macrophytes in 9 of the 11 localities (Fig. 4, Table 1).

Grouping of shell colors extending from RGB data demonstrated that yellow-orange phenotypes were most common ($\bar{x}$ = 58.3%, range among localities 5.9–96.2), followed by brown ($\bar{x}$ = 40.4%, range 6.5–95.1) and olive ($\bar{x}$ = 1.3%, range 0–7.8). At Gulf Shore, North Shore, Merigomish, and Arichat Harbour, yellow-orange frequencies were significantly less common on the invasive than on *F. vesiculosus,* while at Arichat Point yellow-orange were significantly less common on *A. nodosum* (Fig. 5). One locality (Arisaig) showed the opposite with higher frequencies on *F. serratus* relative to *A. nodosum*. The remaining five localities showed no statistical effects or trends.

Multivariate (PCA) integration of the six color space components (R, G, B, H, S, and V) also differentiated the periwinkles among the macrophytes and largely provided parallel or accentuated trends to the categorical RGB analyses. PC1 accounted for 62% of the variance with highest (>0.9) positive loadings for R, G, and V; these corresponded to increased occurrence of yellow-orange shells, while lower PC1 values indicate increased occurrence of dark brown shells. Periwinkles on the invasive macrophyte had significantly lower PC1 values in 6 of 11 localities but higher values (increased yellow-orange) on *A. nodosum* in a single locality (Main a Deux) (Fig. 6). PC2 accounted for 25% of the variance with highest positive loading (0.97) to saturation(S). Periwinkles on the invasive macrophyte had significantly higher PC2 values in five localities and significantly lower values in two localities (Merigomish, Arisaig) (Fig. 7). Scatterplots of PC1 against PC2 for each locality (Supplementary Fig. S1) showed extensive variation among individuals on each macrophyte. Raw data for separate H, S, and V channels are shown in Supplementary Fig. S2.

We also tested whether there were differences in the extent of modality within the frequency distributions of shell hues between the invasive and native macrophytes. While the distributions were "lumpy," our data showed no significant evidence of statistical modality ($\bar{b} > 0.56$) or informative differences among the macrophytes (*F. serratus,* $\bar{b} = 0.40$; *F. vesiculosus,* $\bar{b} = 0.44$; *A. nodosum,* $\bar{b} = 0.40$; $F_{[2,21]} = 0.79$, $P = 0.47$).

Among 3991 shells scored for protoconch color, 28% exhibited a white-spiral phase, 44% were opaline (no spiral), while 28% were the same color as the rest of the shell, ranging from yellow-orange to dark-brown. Frequencies of the white-spiral phase on the invasive macrophyte differed from those on *F. vesiculosus* and *A. nodosum* but not in any consistent manner among localities. In four localities (Gulf Shore, Cape John, Arichat Point, and Main a Deux), the white spiral is significantly less common on the invasive than the native macrophytes, while in two localities (Merigomish, Arisaig), the white spiral is significantly more common (Fig. 8).

Average adult shell size (top 5) was 10.4 mm and differed among the 11 localities (range 9.1–11.8, $F_{[10,119]} = 26.9$, $P < 0.001$). In the five localities where statistically significant differences were observed, shells on *F. serratus* were larger than those on *F. vesiculosus* or *A. nodosum* (Fig. 9).

Carbon and nitrogen stable isotope data indicated that in each locality, periwinkles on *F. serratus* differed from those on *F. vesiculosus* and/or *A. nodosum* (Fig. 10). At North Shore (Fig. 10A) and Arisaig (Fig. 10C), δ^{13}C signatures were lower than on the other macrophytes, while δ^{15}N signatures were higher on *A. nodosum*. At Cape John (Fig. 10B), δ^{13}C signatures were lower and δ^{15}N signatures were higher on *F. vesiculo-*

Fig. 4. Relative occurrence (residuals) of young periwinkles (thin lip) on different macrophytes from collection sites. Localities sorted from west to east. Number at the end of each locality name indicates relative wave exposure (lowest = 1). Stars indicate statistical probability ($^{*}P < 0.05$; $^{**}P < 0.001$) based on 2 × 2 χ^2 test on raw numbers of young and adult periwinkles on *A. nodosum* vs. *F. serratus* and for *F. vesiculosus* vs. *F. serratus*.

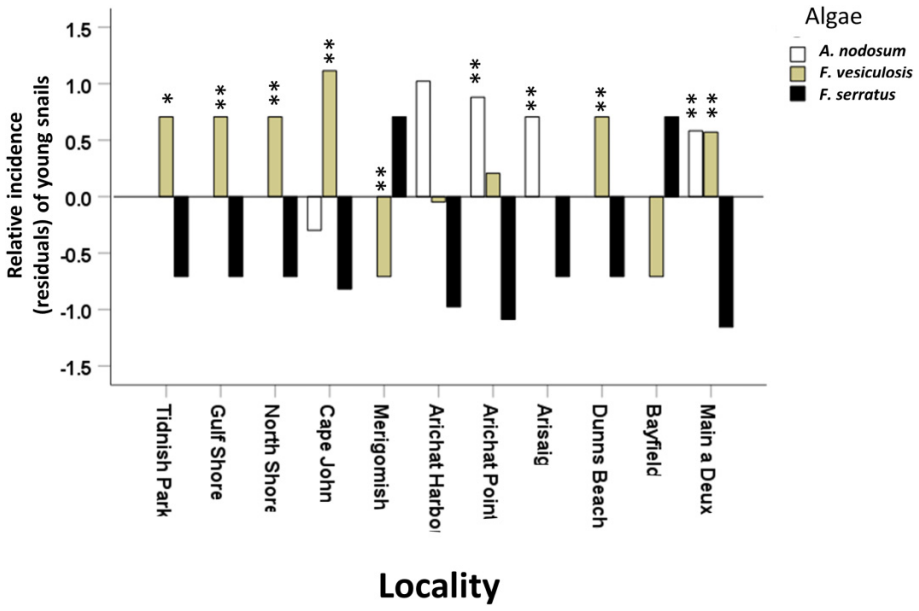

Table 1. Raw data for *L. obtusata* collections among macrophytes for 11 localities in Nova Scotia.

	A. nodosum			*F. vesiculosus*			*F. serratus*			
Locality	$\bar{x}$ mm	Njuv	Nadult	$\bar{x}$ mm	Njuv	Nadult	$\bar{x}$ mm	Njuv	Nadult	*Exp*
Tidnish Park				9.61	34	81	10.5	12	71	3
Gulf Shore				9.8	105	47	10.5*	47	113	3
North Shore				10.5	141	86	10.9*	88	112	3
Cape John	9.1	107	46		151		9.5	160	93	1
Merigomish				11.0	231	245	10.7	255	169	2
Arichat Harbor	10.2	17	80	10.5	12	85	11.0	6	70	2
Arichat Point	9.7	46	17	10.7	33	49	10.3*	18	53	3
Arisaig	11.8	67	216				11.5	10	136	3
Dunns Beach				11.5	78	62	11.3	42	81	4
Bayfield				9.8	184	280	9.8	136	208	3
Main a Deux	11.0	94	51	10.7	147	81	11.5*	11	81	3

Notes: Columns show $\bar{x}$ mean adult shell diameter (top 5), Njuv—number of juvenile periwinkles (thin lip), Nadult—number of adult periwinkles (thick lip). Localities organized from west to east in Nova Scotia. *Exp*—wave exposure (1 = lowest). * indicates $P < 0.05$ of shell size between *F. serratus* and *F. vesiculosus* or *A. nodosum* (Mann–Whitney *U* test).

sus and on *A. nodosum,* compared to the invasive. At Bayfield (Fig. 10D), δ^{15}N signatures were similar for periwinkles on all macrophytes, but δ^{13}C signatures were higher on the invasive than on *F. vesiculosus.* Partitioning age classes of periwinkles showed similar isotopic differences among the macrophytes for juvenile and adults (Figs. 10A–10D).

Discussion

The common lower intertidal macrophyte *F. serratus* from western Europe was introduced to Nova Scotia in the 19th century where it subsequently spread (Johnson et al. 2012; Garbary et al. 2021). We examined whether the intertidal gastropod, *L. obtusata*, typically found on the higher intertidal macrophytes, *F. vesiculosus*, and *A. nodosum,* in both the eastern and western Atlantic would expand its grazing to include the lower intertidal invasive and if so, identify any phenotypic differentiation of the periwinkle on the invasive relative to the adjacent native macrophytes.

Our field data demonstrate that *L. obtusata* is found on the invasive algae with densities generally comparable to those on the native macrophytes. However, we identified marginally lower abundance of juvenile periwinkles on the invasive suggesting a less-preferred substrate for egg deposition or possibly higher mortality of eggs and newly hatched periwinkles. In the UK, *L. obtusata* preferentially lays eggs on *F. vesiculosus* and *A. nodosum* rather than on *F. serratus* (Reimchen 1974) and while we could not confirm that egg masses on

Fig. 5. Percentage of yellow-orange color morphs on different macrophytes from collection sites. Stars indicate statistical probability (*$P < 0.05$; **$P < 0.001$) based on 2×2 χ^2 test on raw numbers of yellow-orange versus brown morphs on *A. nodosum* vs. *F. serratus* and for *F. vesiculosus* vs. *F. serratus*. Scatterplot for raw RGB data shown in Supplementary Figs. 1 A, B, and C.

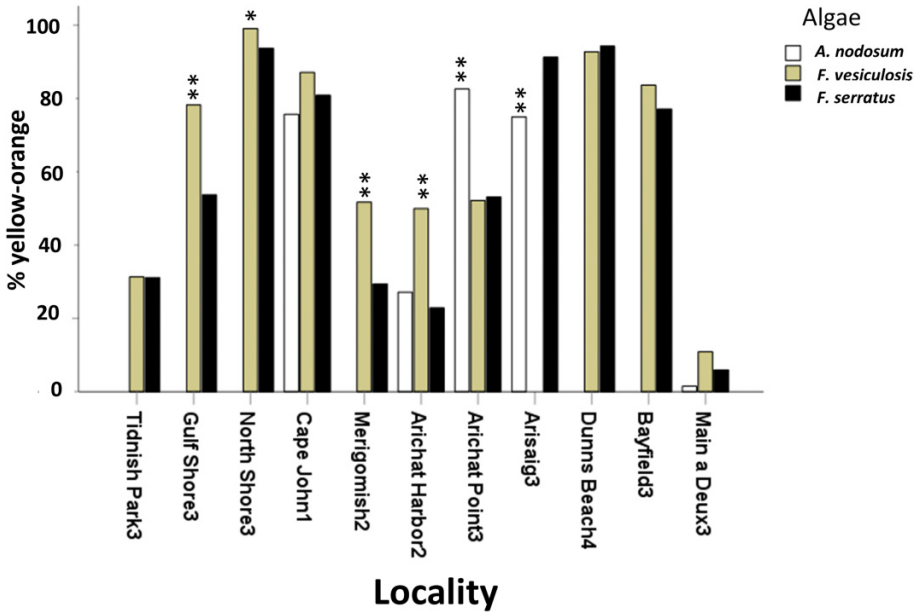

Fig. 6. Principle component scores (PC1—62% of variance) extracted from color (RGB, HSV) of shells on different macrophytes separated for locality. Probability (*$P < 0.05$; **$P < 0.001$) based on separate Analysis of variance of PC1 of periwinkles on *A. nodosum* and/or *F. vesiculosus* against F. *serratus*.

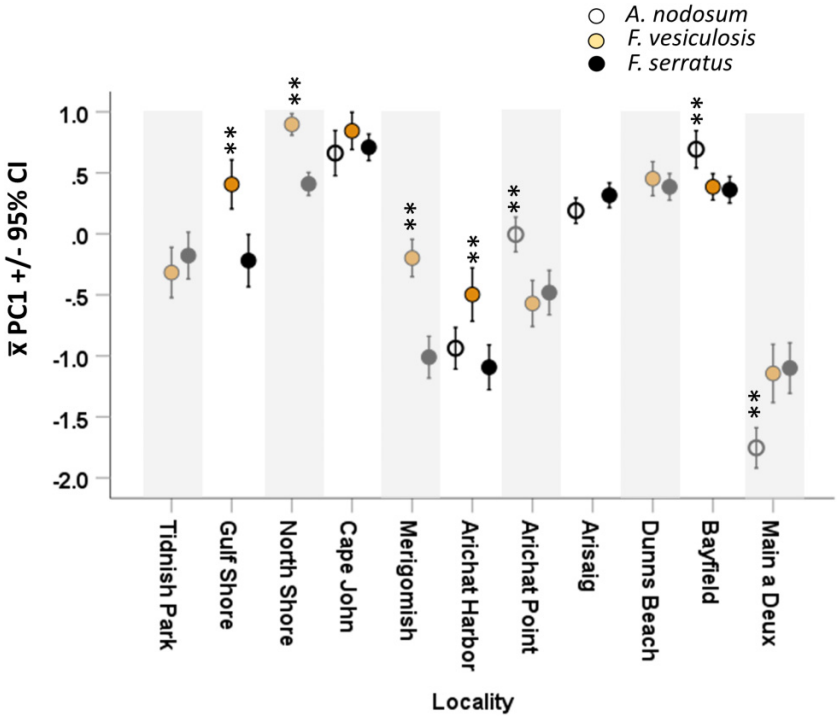

the invasive belonged to *L. obtusata*, the presence of juveniles as well as adults is consistent with residency throughout ontogeny rather than temporary occupation.

An additional factor that supports regular occupation on the invasive emerges from carbon and nitrogen stable isotope data of muscle tissues of the periwinkles. These data provide a proxy for time-integrated diet, the duration dependent on the stability of tissues, and rate of tissue turnover (Vander Zanden and Rasmussen 1999; Casey and Rustad 2016). For muscle in *Littorina,* this ranges from 3 to 8 months (Kemp

Fig. 7. Principle component scores (PC2—25% of variance)) extracted from color (RGB, HSV) of shells on different macrophytes separated for locality. Probability (*$P < 0.05$; **$P < 0.001$) based on separate Analysis of variance of PC1 of periwinkles on *A. nodosum* and/or *F. vesiculosus* against *F. serratus*.

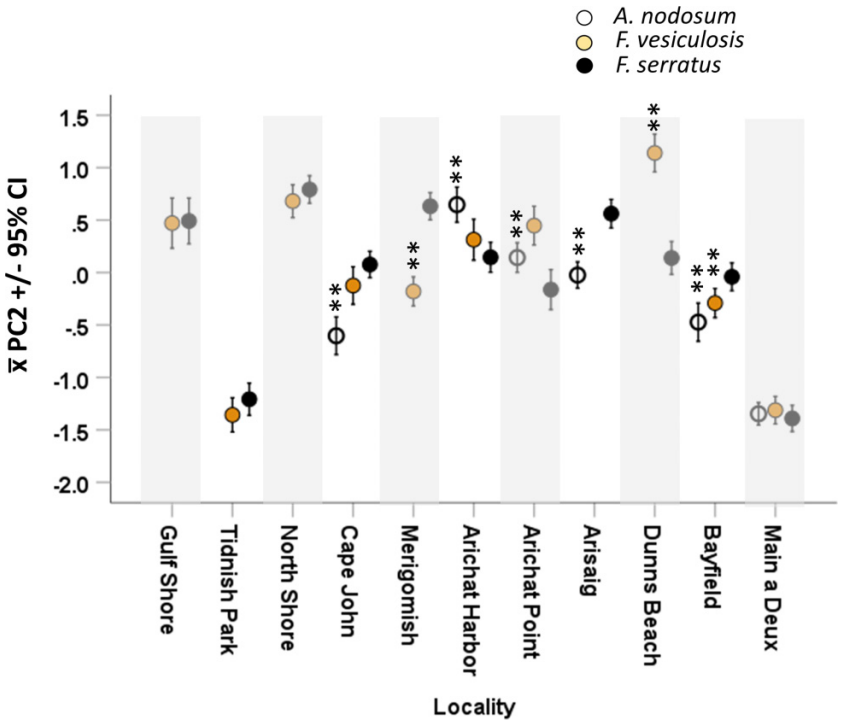

Fig. 8. Frequency of white-spiral phase of the protoconch on *L. obtusata* in relation to macrophyte and locality in Nova Scotia. Probability (*$P < 0.05$; **$P < 0.001$) based on separate χ^2 tests on raw numbers comparing incidence of white-spiral phase on *A. nodosum* and/or *F. vesiculosus* against F. *serratus*.

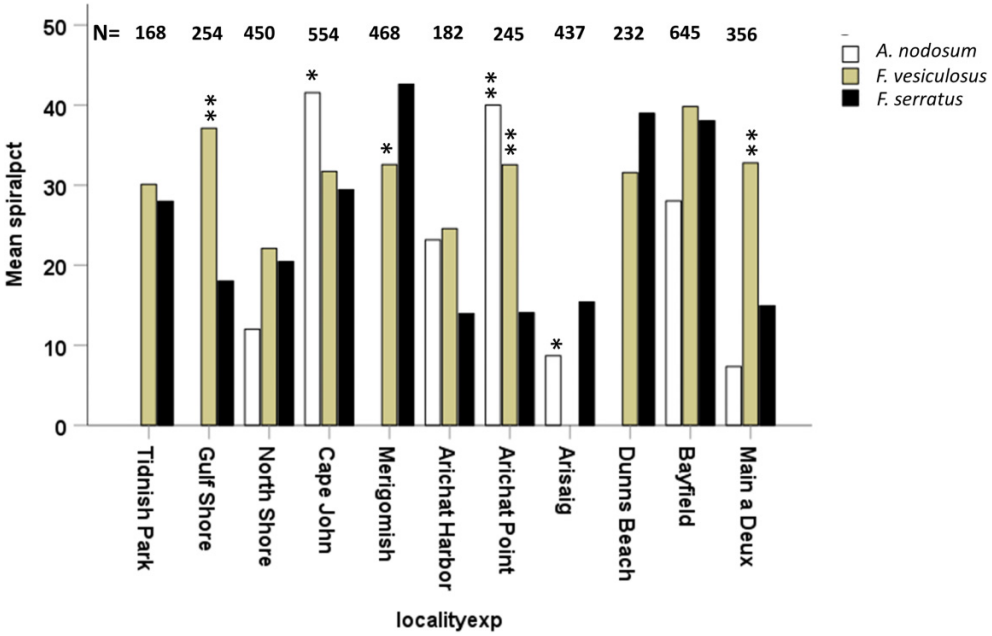

et al. 1990; McIntyre and Flecker 2006). Because macrophyte species differ in the extent of isotopic enrichment, largely due to locality rather than species effects (Viana and Bode 2013, 2015), any grazing fidelity to a specific macrophyte would be reflected in different signatures of the periwinkles among the macrophytes. This was confirmed as in each of the four localities where isotopic data were obtained, we found that either δ^{13}C or δ^{15}N *signatures* of *L. obtusata* on the invasive *F. serratus* differed substantially from those found on the other macrophytes although the direction and extent of en-

Fig. 9. Average adult shell size (top 5) on different macrophytes from collection sites. Probability ($^{*}P < 0.05$; $^{**}P < 0.001$) based on Mann–Whitney *U* for separate comparisons of *A. nodosum* and *F. vesiculosus* against *F. serratus*.

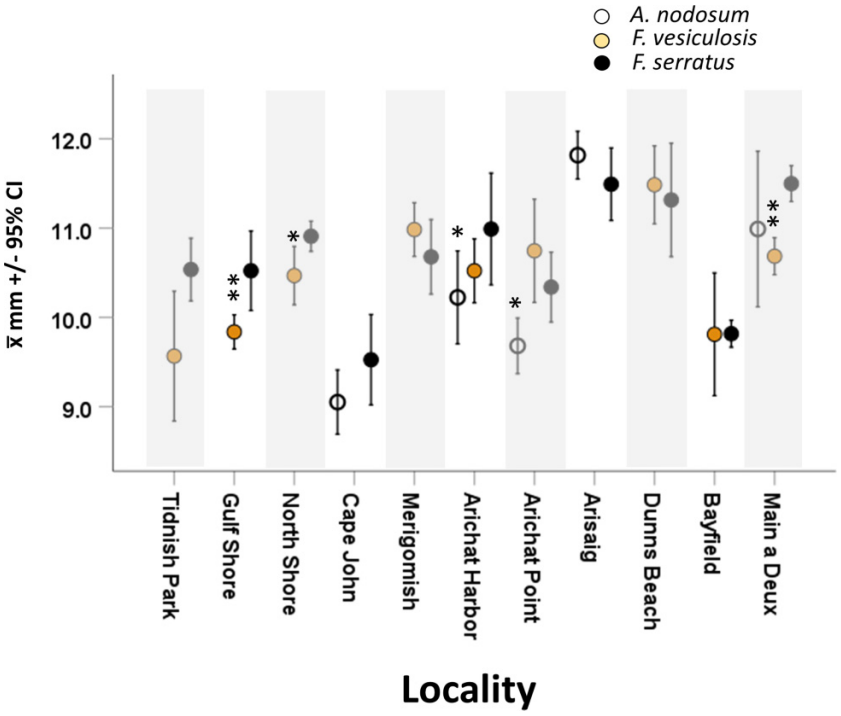

richment differed among the localities. That these differences also occurred among the juvenile age classes further supports residency during early ontogeny.

A second purpose of our study was to quantify shell color differentiation between periwinkles on the invasive versus the adjacent native macrophytes. We suspected that any shell color differentiation on the invasive should be an increase in brown or yellow relative to those on the native macrophytes, as these are the dominant phenotypes on *F. serratus* in the UK and Ireland (Reimchen 1974). *F. serratus* has a distinctive morphology relative to the other macrophytes including a robust dark brown opaque stem and thin, broad, flat olive-brown fronds that lack vesicles. As such, during submergence, *F. serratus* lies close to the substrate rather than projecting into the water column as do *F. vesiculosus* and *A. nodosum,* both of which have vesicles on the fronds (Reimchen 1974, 1979 and unpublished observations). The dark reticulata morph of *L. fabalis* is exceptionally camouflaged on the opaque stem while the yellow morph is very conspicuous on the stem and fronds. Yet, when the periwinkles are viewed from a common hunting position of intertidal fish that prey on the periwinkles, that is, from beneath the fronds, the light transmitted through the thin fronds appears bright yellow and the yellow shells on the underside of the fronds are highly camouflaged (Fig. 3C: Reimchen 1979). Fronds of *F. vesiculosus* and *A. nodosum* are thicker, resulting in very limited light transmission and as such remain largely olive or brown, although younger fronds are often yellow. Our results were moderately consistent with this prediction as in one-half of the localities, shells on *F. serratus* were significantly darker (brown) or lighter (yellow) than those on the native macrophytes. This is not a consequence of frequency shifts of discrete morphs but rather frequency changes in the distribution of quantitative (continuous) shell color traits. Such shifts could be due to differences in the spectral backgrounds of *F. serratus* extending from the relative abundance of juvenile snails on the stem versus the fronds that varies among localities (Reimchen 1979). As well, the lower intertidal position of *F. serratus* receives less illumination than upper intertidal zones, particularly at longer wavelengths, which attenuate rapidly in surface waters (Paulson and Simpson 1977). These factors would presumably influence their detection by aquatic visual predators.

The differences in frequency of shell color phenotypes we observed occurred over a maximum of about one century and while we assume these are adaptive responses, we do not know whether this represents phenotypic plasticity or heritable effects. Previous studies indicate genetic control of pigment expression to the background hue of *L. obtusata* shells (Kozminsky 2014), while breeding experiments using *L. fabalis* suggest Mendelian segregation of the major shell morphs (Reimchen 1979).

In the UK and Ireland, shells of *L. fabalis* on *F. serratus* are usually yellow (morph citrina) or brown and patterned (morph light or dark reticulata) and rarely olive (morph olivacea) is rare. Consequently, we predicted that in our study sites in Atlantic Canada, the olive phenotype would be less common on *F. serratus.* We found this to be the case but unexpectedly, our results showed that the olive shell color, the most common phenotype of *L. obtusata* in Western Europe, was uncommon or absent on all macrophytes from Nova Scotia. This phenotype is common in Maine close to Nova Scotia

Fig. 10. Stable isotope signatures of *L. obtusata* muscle tissue collected on different macrophytes from four localities in Nova Scotia. Each point on graph is a different periwinkle. Note differences in scales among plots. Letters beside each symbol differentiate size class of periwinkle (A = adult, J = juvenile).

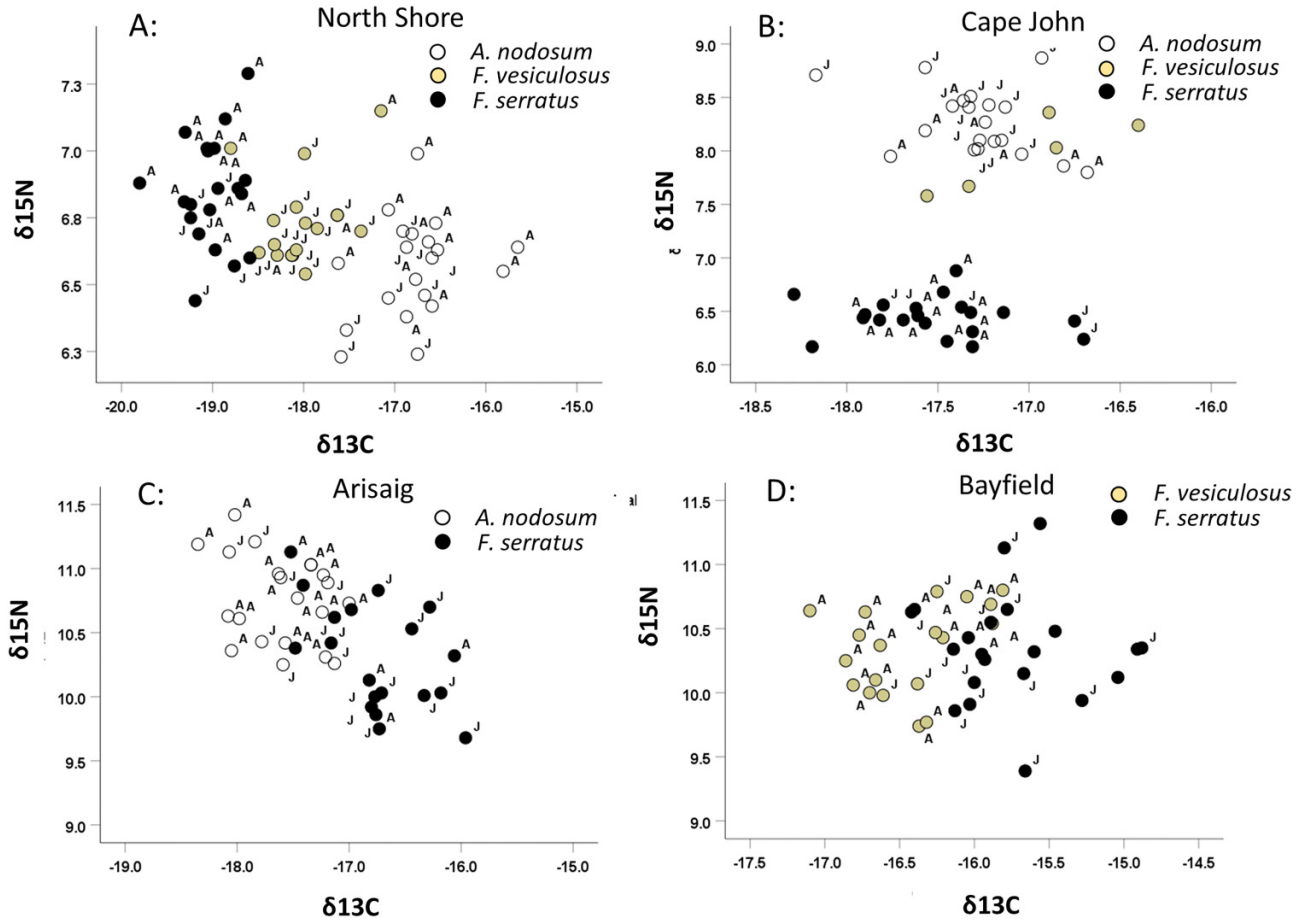

(Phifer-Rixey et al. 2008). At present, we cannot account for this trend.

We also evaluated color of the shell apex which often differs from the major shell whorl color. On older shells, the apex can be abraded and pale in appearance independent of the color of the major whorl, but on younger periwinkles, the apex is not abraded and directly reflects the early post-hatching protoconch color. Breeding experiments are consistent with genetic control of the white-spiral banding (Reimchen 1989; Kozminsky 2016). We observed the white-spiral phenotype in most localities, six of which had lower incidence of the white spiral on the invasive, while two localities showed increased occurrence. In the UK and Ireland, the white spiral phase on *L. fabalis* is prevalent in association with high densities of the tube-dwelling polychaete *Spirorbis borealis* (Daudin, 1800) found cemented to the algal fronds and has an advantage relative to shells without the white spiral in predation experiments (Reimchen 1989). We did not record the abundance of *Spirorbis* in our study although it is known that in Atlantic Canada, *Spirorbis* is common on *F. vesiculosus* but can vary among localities (Doyle 1974). Such differences may contribute to the locality and macrophyte differences that we observed in the occurrence of the white-spiral phase. For example, at Merigomish, where the white-spiral phase was relatively more abundant on *F. serratus* than on *F. vesiculosis,* the shore substrate was composed of extensive mud and fine silt, a substrate that facilitates *Spirorbis* abundance in the east Atlantic (OConner and Lamont 1978; Reimchen 1981). In contrast, at Main a Deux, the white-spiral phase was much less common on *F. serratus* than on *F. vesiculosis* and in this locality, the substrate was predominantly small boulders and pebbles, differences that could simply reflect reduced habitat suitability for *Spirorbis.*

An additional component that differentiates *L. obtusata* from *L. fabalis* in western Europe is the discreteness of the shell colors, those of *L. obtusata* showing a more continuous distribution of hues compared with the more discrete color morphs of *L. fabalis,* with these differences corresponding to the dominant substrate hues of the different macrophytes (Reimchen 1974). The evolution of polymorphic traits is facilitated by selection against intermediate phenotypes that can occur if there are distinct microhabitats (Ford 1963; Villoutriex et al. 2023), as is the case with *F. serratus* (Reimchen 1979). The bimodality coefficients of shell colors that we quantified for shells on each macrophyte approached statistical significance, but there were no differences in the extent of

modality among the macrophytes and as such no current evidence to suggest increased disruptive selection on shell hue of the periwinkles occupying the invasive.

A further morphological distinction between *L. obtusata* and *L. fabalis* in western Europe is adult shell diameter, the former being substantially larger than the latter (~15 mm vs. ~10 mm, respectively) (Sacchi 1969). Consequently, we predicted that if there was evidence of phenotypic adaptation in the direction of *L. fabalis*, *L. obtusata* would exhibit a smaller adult shell on the lower intertidal invasive relative to the native macrophytes. Our results were opposite as the shells were significantly larger on *F. serratus* in 5 of the 11 localities. This trend is more consistent with that observed in some shores of the United Kingdom where adult shells of *L. obtusata* are larger at lower intertidal zones, probably associated with defense against large crab predators that are prevalent in the lower intertidal zone (Vermeij 1976; Reimchen 1982; Palmer 1985; reviews in Vermeij 1993; Dalziel and Boulding 2005; Pascoal et al. 2012). It is interesting to note, however, that the average adult sizes of *L. obtusata* in our study (10.4 mm) as well as 87 other localities in Nova Scotia and Newfoundland ($\bar{x} = 10.5$ mm; Reimchen, unpublished data) are similar to the average adult sizes of *L. fabalis* in western Europe (10.0 mm) rather than that of *L. obtusata* (Reimchen 1982). Such small adult shell sizes might represent phenotypic plasticity in response to environmental cues such as wave action (Trussell 2000; Brookes and Rochette 2007; Bourdeau et al. 2015). Alternatively, the extensive winter ice-scouring of intertidal zones in the northwestern Atlantic compared to the more moderate climate of the eastern Atlantic (Petzold et al. 2014) could be expected to limit longevity and shell size of the macrophyte-dependent *L. obtusata*. Small adult size can also be favoured by microspatial differences in size classes of crabs in the intertidal that can result in divergent selection for small versus large adult shells (Reimchen 1982).

Emerging studies on multiple taxa demonstrate that phenotypic and genotypic differentiation can occur in short time periods such as decades particularly where new selective landscapes are highly distinctive (Hendry and Kinnison 1999; Callaway and Maron 2006; Strauss et al. 2006; Leaver and Reimchen 2012; Marques et al. 2018). Our data demonstrate that a common intertidal periwinkle in Atlantic Canada has expanded its foraging niche to include a new invasive macrophyte on which it has differentiated in shell color and adult shell size relative to conspecifics from adjacent native macrophytes. These are still early stages of a potential complex of phenotypic adaptations that periwinkles exhibit on *F. serratus* in western Europe where the macrophyte is native (Sacchi 1969; Reimchen 1974, 1981, 1982; Goodwin and Fish 1977). Furthermore, the recent invasion of the predatory green crab (*Carcinus maenus* (Linnaeus, 1758)) to the western Atlantic has led to morphological differences in shell size of *L. littorea* (Linnaeus) (Vermeij 1982; Edgell and Rochette 2008). In the eastern Atlantic, this crab is a major predator on *L. obtusata* and *L. fabalis* (Reimchen 1982). That the invasive macrophyte *F. serratus* and *C. maenus* are still expanding in the western Atlantic (Johnson et al. 2012) creates a novel selective landscape for *L. obtusata* and raises the possibility of identifying a time series for phenotypic and genomic differentiation in a direction predicted by adaptations of *L. fabalis* on F. *serratus* in western Europe.

Acknowledgements

We thank S.D. Douglas, J.&L. Buckland-Nicks for field assistance, K. Cox for programming assistance in image analyses, S. Duckett for scoring protoconch color, and S.D. Douglas for edits on the manuscript. Author contributions: TER—conceptual development, field collections, analyses, manuscript preparation, and supervision; ARBC—imaging, shell color, and size quantification, and manuscript contributions; JH—imaging, shell color and size quantification, isotope analyses, and manuscript contributions. Travel support and field expenses for TER occurred when in receipt of the James Chair professorship (1995) at St Francis Xavier University, Nova Scotia. The research was additionally supported by a Natural Sciences and Engineering Council of Canada Research operating grant to the TER (NRC2354). Raw data will be available on reasonable request to the corresponding author. R-scripts are available on https://doi.org/10.6084/m9.figshare.25457914Can or by using the following web link: https://figshare.com/account/home#/projects/199408.

Article information

History dates

Received: 28 January 2024
Accepted: 31 March 2024
Accepted manuscript online: 6 May 2024
Version of record online: 7 August 2024

Copyright

Author information

Author ORCIDs

T.E. Reimchen https://orcid.org/0000-0002-5578-8531

Author contributions

Conceptualization: TER
Data curation: TER
Formal analysis: TER, JH, ARBC
Funding acquisition: TER
Investigation: TER, JH, ARBC
Methodology: TER, JH, ARBC
Project administration: TER
Software: ARBC
Supervision: TER
Validation: TER
Visualization: TER, ARBC
Writing – original draft: TER
Writing – review & editing: TER, JH, ARBC

Competing interests

The authors declare there are no competing interests.

Supplementary material

Supplementary data are available with the article at https://doi.org/10.1139/cjz-2024-0018.

References

Bourdeau, P.E., Butlin, R.K., Bronmark, C., Edgell, T.C., Hoverman, J.T., and Hollander, J. 2015. What can aquatic gastropods tell us about phenotypic plasticity? A review and meta-analysis. Heredity, **115**: 312–321. doi:10.1038/hdy.2015.58. PMID: 26219231.

Brookes, J.L., and Rochette, R. 2007. Mechanism of a plastic phenotypic response: predator-induced shell thickening in the intertidal gastropod *Littorina obtusata*. J. Evol. Biol. **20**: 1015–1027. doi:10.1111/j.1420-9101.2007.01299.x. PMID: 17465912.

Callaway, R.M., and Maron, J.L. 2006. What have exotic plant invasions taught us over the past 20 years? Trends Ecol. Evol. **21**: 369–374. doi:10.1016/j.tree.2006.04.008. PMID: 16815436.

Casey, W.H., and Rustad, J.R. 2016. Pathways for oxygen-isotope exchange in two model oxide clusters. New J. Chem. **40**: 898–905. doi:10.1039/C5NJ00985E.

Cox, K.D., Woods, M.B., and Reimchen, T.E. 2021. Regional heterogeneity in coral species richness and hue reveals novel global predictors of reef fish intra-family diversity. Sci. Rep. **11**: 1–12. doi:10.1038/s41598-021-97862-8. PMID: 33414495.

Dalziel, B., and Boulding, E.G. 2005. Water-borne cues from a shell-crushing predator induce a more massive shell in experimental populations of an intertidal periwinkle. J. Exp. Mar. Biol. Ecol. **317**: 25–35. doi:10.1016/j.jembe.2004.11.015.

Dijkstra, J.A., Harris, L.G., Mello, K., Litterer, A., Wells, C., and Ware, C. 2017. Invasive seaweeds transform habitat structure and increase biodiversity of associated species. J. Ecol. **105**: 1668–1678. doi:10.1111/1365-2745.12775.

Doyle, R.W. 1974. Choosing between darkness and light: the ecological genetics of photic behaviour in the planktonic larva of *Spirorbis borealis*. Mar. Biol. **25**: 311–317. doi:10.1007/BF00404973.

Edelstein, T., Greenwell, M., Bird, C.J., and McLachlan, J. 1973. Investigations of the marine algae of Nova Scotia. X. Distribution of *Fucus serratus* L. and some other species of *Fucus* in the Maritime Provinces. Proc. Nova Scotian Inst. Sci. **27**: 33–42.

Edgell, T.C., and Rochette, R. 2008. Differential periwinkle predation by an exotic crab and the geography of shell-claw covariance in the northwest Atlantic. Evolution, **62**: 1216–1228. doi:10.1111/j.1558-5646.2008.00350.x. PMID: 18298647.

Endler, J.A. 1991. Variation in the appearance of guppy color patterns to guppies and their predators under different visual conditions. Vision Res. **31**: 587–608. doi:10.1016/0042-6989(91)90109-I. PMID: 1843763.

Ford, E.B. 1963. Ecological genetics. London, Methuen.

Garbary, D.J., Fass, M.P., and Vandermeulen, H. 2021. Invasive *Fucus serratus* (Fucaceae, Phaeophyceae) responds to climate change along the Atlantic Coast of Nova Scotia, Canada. Bot. Mar. **64**: 407–417. doi:10.1515/bot-2021-0056.

Goodwin, B.J., and Fish, J.D. 1977. Inter-and intraspecific variation in *Littorina obtusata* and *L. mariae* (Gastropoda: Prosobranchia). J. Molluscan Stud. **43**: 241–254. http://mollus.oxfordjournals.org/

Hendry, A.P., and Kinnison, M.T. 1999. Perspective: the pace of modern life: measuring rates of contemporary microevolution. Evolution, **53**: 1637–1653. doi:10.1111/j.1558-5646.1999.tb04550.x. PMID: 28565449.

Johnson, L.E., Brawley, S.H., and Adey, W.H. 2012. Secondary spread of invasive species: historic patterns and underlying mechanisms of the continuing invasion of the European rockweed *Fucus serratus* in eastern North America. Biol. Invasions **14**: 79–97. doi:10.1007/s10530-011-9976-z.

Kemp, P.F., Newell, S.Y., and Hopkinson, C.S. 1990. Importance of grazing on the salt-marsh grass *Spartina alterniflora* to nitrogen turnover in a macrofaunal consumer, *Littorina irrorata*, and to decomposition of standing-dead *Spartina*. Mar. Biol. **104**: 311–319. doi:10.1007/BF01313273.

Knapp, T.R. 2007. Bimodality revisited. J. Mod. Appl. Stat. Methods, **6**: 3. doi:10.22237/jmasm/1177992120.

Kozminsky, E.V. 2014. Inheritance of the background shell color in the periwinkles *Littorina obtusata* (Gastropoda, Littorinidae). Russ. J. Genet. **50**: 1038–1047. doi:10.1134/S1022795414100044.

Kozminsky, E.V. 2016. Inheritance of longitudinal white shell bands in the periwinkle *Littorina obtusata* (Gastropoda, Prosobranchia). Russ. J. Genet. **52**: 882–886. doi:10.1134/S1022795416080068.

Leaver, S.D., and Reimchen, T.E. 2012. Abrupt changes in defense and trophic morphology of the giant threespine stickleback (*Gasterosteus* sp.) following colonization of a vacant habitat. Biol. J. Linn. Soc. **107**: 494–509. doi:10.1111/j.1095-8312.2012.01969.x.

Levine, J.M., Vila, M., Antonio, C.M.D., Dukes, J.S., Grigulis, K., and Lavorel, S. 2003. Mechanisms underlying the impacts of exotic plant invasions. Proc. Royal Soc. B. **270**: 775–781. doi:10.1098/rspb.2003.2327.

Marques, J.P., Sotelo, G., Larsson, T., Johannesson, K., Panova, M., and Faria, R. 2017. Comparative mitogenomic analysis of three species of periwinkles: *Littorina fabalis*, *L. obtusata* and *L. saxatilis*. Mar. Genomics, **32**: 41–47. doi:10.1016/j.margen.2016.10.006.

Marques, D.A., Jones, F.C., Di Palma, F., Kingsley, D.M., and Reimchen, T.E. 2018. Experimental evidence for rapid genomic adaptation to a new niche in an adaptive radiation. Nat. Ecol. Evol. **2**:1128–1138. doi:10.1038/s41559-018-0581-8. PMID: 29942074.

McIntyre, P.B., and Flecker, A.S. 2006. Rapid turnover of tissue nitrogen of primary consumers in tropical freshwaters. Oecologia, **148**: 12–21. doi:10.1007/s00442-005-0354-3. PMID: 16456686.

O'Connor, R. J., and Lamont, P. 1978. The spatial organization of an intertidal *Spirorbis* community. J. Exp. Mar. Biol. Ecol. **32**: 143–169. doi:10.1016/0022-0981(78)90112-0.

Palmer, A.R. 1985. Adaptive value of shell variation in *Thais lamellosa*: effect of thick shells on vulnerability to and preference by crabs. Veliger, **27**: 349–356.

Pascoal, S., Carvalho, G., Creer, S., Mendo, S., and Hughes, R. 2012. Plastic and heritable variation in shell thickness of the intertidal gastropod *Nucella lapillus* associated with risks of crab predation and wave action, and sexual maturation. PLoS ONE, **7**: e52134. doi:10.1371/journal.pone.0052134. PMID: 23272221.

Paulson, C.A., and Simpson, J.J. 1977. Irradiance measurements in the upper ocean. J. Phys. Oceanogr. **7**: 952–956. doi:10.1175/1520-0485(1977)007⟨0952:IMITUO⟩2.0.CO;2.

Petzold, W., Willers, M.T., and Scrosati, R.A. 2014. Visual record of intertidal disturbance caused by drift ice in the spring on the Atlantic coast of Nova Scotia. F1000Research **3**. doi:10.12688/f1000research.4146.1.

Phifer-Rixey, M., Heckman, M., Trussell, G.C., and Schmidt, P.S. 2008. Maintenance of clinal variation for shell colour phenotype in the flat periwinkle *Littorina obtusata*. J. Evol. Biol. **21**: 966–978. doi:10.1111/j.1420-9101.2008.01549.x. PMID: 18507701.

Reimchen, T.E. 1974. Studies on the biology and color polymorphism of two sibling species of marine gastropod (Littorina). Ph.D. thesis. University of Liverpool, Liverpool, England.

Reimchen, T.E. 1979. Substratum heterogeneity, crypsis, and color polymorphism in an intertidal periwinkle (*Littorina mariae*). Can. J. Zool. **57**: 1070–1085. doi:10.1139/z79-135.

Reimchen, T.E. 1981. Microgeographical variation in *Littorina mariae* Sacchi & Rastelli and a taxonomic consideration. J. Conchol. **30**: 341–350.

Reimchen, T.E. 1982. Shell size divergence in *Littorina mariae* and *L. obtusata* and predation by crabs. Can. J. Zool. **60**: 687–695. doi:10.1139/z82-098.

Reimchen, T.E. 1989. Shell color ontogeny and tubeworm mimicry in a marine gastropod *Littorina mariae*. Biol. J. Linn. Soc. **36**: 97–109. doi:10.1111/j.1095-8312.1989.tb00485.x.

Sacchi, C.F. 1969. Research on comparative ecology of *Littorina-obtusata* (L) and *Littorina-mariae* Sacchi and Rastelli (Gastropoda, Prosobranchia) in Galicia and Brittany. Invest. Pesq. **33**: 381.

Sacchi, R., Pellitteri-Rosa, D., Bellati, A., Di Paoli, A., Ghitti, M., Scali, S., et al. 2013. Colour variation in the polymorphic common wall lizard (*Podarcis muralis*): an analysis using the RGB colour system. Zool. Anz. **252**: 431–439. doi:10.1016/j.jcz.2013.03.001.

Sotelo, G., Duvetorp, M., Costa, D., Panova, M., Johannesson, K., and Faria, R. 2020. Phylogeographic history of flat periwinkles, *Littorina fabalis* and *L. obtusata*. BMC Evol. Biol. **20**: 1–18. doi:10.1186/s12862-019-1561-6. PMID: 31906845.

Strauss, S.Y., Lau, J.A., and Carroll, S.P. 2006. Evolutionary responses of natives to introduced species: what do introductions tell us about

natural communities? Ecol. Lett. **9**: 357–374. doi:10.1111/j.1461-0248.2005.00874.x. PMID: 16958902.

Trussell, G.C. 2000. Predator-induced plasticity and morphological trade-offs in latitudinally separated populations of *Littorina obtusata.* Evol. Ecol. Res. **2**: 803–822.

Valvo, J.J., Aponte, J.D., Daniel, M.J., Dwinell, K., Rodd, H., Houle, D., and Hughes, K.A. 2021. Using Delaunay triangulation to sample whole-specimen color from digital images. Ecol. Evol. **11**: 12468–12484. doi:10.1002/ece3.7992. PMID: 34594513.

Vander Zanden, M.J., and Rasmussen, J.B. 1999. Primary consumer δ 13 C and δ 15 N and the trophic position of aquatic consumers. Ecology, **80**: 1395–1404. https://www.jstor.org/stable/177083. doi:10.1890/0012-9658(1999)080%5b1395:PCCANA%5d2.0.CO;2.

Van Volkom, K.S., Harris, L.G., and Dijkstra, J.A. 2021. The influence of invasive ascidian diets on the growth of the sea star *Henricia sanguinolenta*. J. Mar. Biol. Assoc. U. K. **101**: 151–157. doi:10.1017/S0025315420001228.

Vermeij, G.J. 1976. Interoceanic differences in vulnerability of shelled prey to crab predation. Nature, **260**: 135–136. doi:10.1038/260135a0.

Vermeij, G.J. 1982. Environmental change and the evolutionary history of the periwinkle (*Littorina littorea*) in North America. Evolution, **1**: 561–580. doi:10.2307/2408101.

Vermeij, G.J. 1993. Evolution and escalation: an ecological history of life. Princeton University Press, Princeton, NJ.

Viana, I.G., and Bode, A. 2013. Stable nitrogen isotopes in coastal macroalgae: geographic and anthropogenic variability. Sci. Total. Environ. **443**: 887–895. doi:10.1016/j.scitotenv.2012.11.065. PMID: 23247291.

Viana, I.G., and Bode, A. 2015. Variability in δ15N of intertidal brown algae along a salinity gradient: differential impact of nitrogen sources. Sci. Total. Environ. **512**: 167–176. doi:10.1016/j.scitotenv.2015.01.019. PMID: 25617782.

Villoutreix, R., De Carvalho, C.F., Feder, J.L., Gompert, Z., and Nosil, P. 2023. Disruptive selection and the evolution of discrete color morphs in *Timema* stick insects. Sci. Adv. **9**: eabm8157. doi:10.1126/sciadv.abm8157. PMID: 37000882.

Watson, D.C., and Norton, T.A. 1987. The habitat and feeding preferences of *Littorina obtusata* (L.) and *L. mariae* Sacchi et Rastelli. J. Exp. Mar. Biol. Ecol. **112**: 61–72. doi:10.1016/S0022-0981(87)80015-1.

Weller, H. 2019. countcolors: locates and counts pixels within color range(s) in images. R package version 0.9.1. Available from https://CRAN.R-project.org/package=countcolors [accessed March 2023].

Weller, H. 2021. colordistance: distance metrics for image color Similarity. R package version 1.1.2.Available from https://CRAN.R-project.org/package=colordistance [accessed March 2023].

Williams, G.A. 1994. Variation in populations of *Littorina obtusata* and *L. mariae* (Gastropoda) in the Severn Estuary. Biol. J. Linn. Soc. **51**: 189–198. doi:10.1111/j.1095-8312.1994.tb00953.x.

Williams, G.A. 1995. Maintenance of zonation patterns in two species of flat periwinkle, *Littorina obtusata* and *L. mariae*. Hydrobiologia, **309**: 143–150. doi:10.1007/BF00014481.